July 1984 LRP 237/84

EFFECT OF RF HEATING ON EDGE PARAMETERS IN THE TCA TOKAMAK

A. de Chambrier, G.A. Collins, P.-A. Duperrex,
A. Heym, F. Hofmann, Ch. Hollenstein, B. Joye,
R. Keller, A. Lietti, J.B. Lister, F.B. Marcus,
J.-M. Moret, S. Nowak, A. Pochelon, W. Simm and
S.Veprek

presented at the
6th International Conference on
PLASMA SURFACE INTERACTIONS IN CONTROLLED FUSION DEVICES
Nagoya, Japan
May 14 - 18, 1984

EFFECT OF RF HEATING ON EDGE PARAMETERS IN THE TCA TOKAMAK

A. de Chambrier, G.A. Collins, P.-A. Duperrex, A. Heym, F. Hofmann, Ch. Hollenstein, B. Joye, R. Keller, A. Lietti, J.B. Lister, F.B. Marcus, J.-M. Moret, S. Nowak*, A. Pochelon, W. Simm and S. Veprek**

Centre de Recherches en Physique des Plasmas
Association Euratom - Confédération Suisse
Ecole Polytechnique Fédérale de Lausanne
21, Av. des Bains, CH-1007 Lausanne/Switzerland

* University of Fribourg, Plasma Physics Department,
CH-1700 Fribourg/Switzerland

** Institute of Inorganic Chemistry, University of Zurich,
CH-8057 Zürich/Switzerland

Abstract

Detailed scrape-off measurements during Alfvén wave heating experiments ($P_{RF} \sim 200$ kW) in TCA are presented. The measurements are performed by means of electrical probes and by deposition probes fixed onto the antennae. It is shown that different antenna designs strongly influence the behaviour of the boundary plasma. Even during low power RF heating experiments it is found that the plasma-antenna interaction leads to a non-Maxwellian plasma. Low frequency density fluctuations are associated with gradient changes of the density and temperature profiles. High frequency fluctuations at the driving frequency and their harmonics are observed.

1. INTRODUCTION

The scrape-off layer has been the subject of many investigations /1,2/. This intensive work has shown that the boundary plasma plays an important role in fusion experiments, which demand strong auxiliary heating to reach their goal. Among the most promising methods, beside neutral beam heating, are the various RF schemes. These RF schemes operate at very different frequencies and use, therefore, various types of antennae which are usually immersed in the scrape-off plasma. This location and the large RF power may lead to adverse plasma-antenna interactions, which produce an impurity influx into the hot plasma core. Little is known of the behaviour of the boundary plasma during intense RF heating /3,4/. Investigations of the scrape-off layer under these conditions are necessary to obtain information on the physics of the boundary plasma behaviour in heating experiments, which is also important for advanced antenna design.

In this study, we present scrape-off measurements during high power Alfvén wave heating experiments in TCA. Alfvén wave heating refers to the resonant absorption of wave energy at a particular layer in the plasma, where the imposed wave phase velocity equals the local value of the Alfvén velocity. This absorption is dominant at frequencies below the ion cyclotron frequency. The scrape-off layer has been diagnosed by means of electrical probes and by passive collection probes fixed on the antenna. We present detailed measurements of the basic scrape-off layer parameters during Alfvén wave heating experiments for two different antenna types used in TCA.

The measurements show that the boundary plasma behaviour is different for the two types of antenna. In both cases, an apparent electron temperature increase is observed. The electron density behaviour is very different for each of the two antennae although a general decrease of the electron density during the RF phase is observed in both. Independently of the antenna type, non-Maxwellian edge plasmas are observed originating from strong plasma-antenna interactions.

The paper is organized in the following way: In section 2, experimental details about the TCA Tokamak and the scrape-off diagnostics are presented. Detailed scrape-off measurements are shown in section 3. Section 4 draws conclusions from these results.

2. EXPERIMENTS

The study of Alfvén wave heating is the main topic of the TCA Tokamak. Its main operating parameters are $R = 0.61$ m, $a = 0.18$ m and $B \leq 15$ kG /5/. The limiter material used is pure carbon with Hydrogen and Deuterium as the filling gas.

In the experiments reported here, the frequency of the RF is fixed at 2.5 MHz. RF power up to 200 kW has been delivered to the plasma during these experiments which approximately equals the ohmic heating power in the target plasma /6/.

The RF antenna structure consists of eight separate antenna groups sited above and below the plasma at four equally-spaced toroidal locations. Two different kinds of antennae have been used in this study. Figure 1a shows one of the eight original antenna groups composed of three stainless steel plate antennae used until the end of 1983 /7/. These antennae were placed about 20 mm behind the limiter radius. In all the investigations presented, no antenna side screens were used. The stainless steel plate antenna represented about 16% of the plasma surface. This antenna was replaced by bar antennae /8/, the mechanical design of which is shown in Fig. 1b. The antenna is constructed out of 10 mm stainless steel bars. In order to reduce the quantity and the ionic charge Z of the sputtered material, we have coated the stainless steel bars with TiN. The TiN layer has a thickness of about 6-7 μm and was deposited using the CVD process. To reduce interaction with the edge plasma, we also increased the antenna plasma spacing from 20 mm to 30 mm.

The scrape-off layer has been investigated by means of electrical probes. A movable Langmuir probe is installed in the equitorial plane of the TCA vacuum vessel. The probe is opposite the limiters and is a 5-mm long Molybdenum wire of 0,6 mm in diameter. The probe voltage can be swept between -100 V and 100 V within about 1 ms. The probe current was measured with a current probe with a frequency response as high as 50 MHz. The ion density is obtained from measurements of the ion saturation current (probe bias -200 V). The electron temperatures were obtained through analyses of the Langmuir probe characteristics. The treatment used assumes that the plasma under investigation is Maxwellian. Hot-electron distributions may complicate this analysis, as we shall show. Density fluctuations are detected by ion saturation current fluctuations and were analysed by a spectrum analyser operated either in the sweep mode or as a narrow band receiver at a fixed frequency.

The ion temperature has been obtained from a fixed Katsumata probe /9/, placed at a distance of 40 mm outside the limiter radius.

It is well-known that probe measurements may be strongly affected by intense RF /10,11/. In our case, no direct RF pick-up on the probe has been found. All the measurements shown in the present work are, however, time averaged over many RF cycles. The present study indicated clearly that RF time-scale resolved measurements are necessary to understand the plasma-antenna interaction in more detail. As we shall show in the next section, it is found that the boundary plasma becomes non-Maxwellian in the presence of intense RF. The interpretation of the probe characteristics of a non-Maxwellian plasma is a much more severe problem than the previous one. In this case, a careful analysis of the measured probe currents is required. Studies in low density plasmas, where probe diagnostics are the main tool, clearly show that even under such conditions useful and important information, such as the beam energy, beam density and tail formation, can be obtained from simple Langmuir traces.

As well as the Langmuir and Katsumata probes, passive deposition probes have been mounted on the stainless steel antennae to determine impurity deposition to the outside of the antenna. Two carefully cleaned Mo-samples were attached on the same antenna plate, one parallel to the main magnetic field and antenna plate and the second perpendicularly oriented to the main field. The insertion of the samples into the Tokamak, their removal and transportation to the XPS apparatus for analysis were done in air but any other contamination was excluded. The samples have been analysed by X-ray photoelectron spectroscopy (XPS) after exposure to about 300 shots.

3. RESULTS

a) Deposition probes

During exposure, the samples experienced daily Taylor discharge cleaning and plasma shots covering the entire operating range of TCA. The samples were analysed by XPS, using AlK_α radiation. The main impurities found after exposure are carbon, iron, chromium and oxygen. Figure 2 shows the XPS spectrum obtained for the two differently oriented samples. We notice that the parallel oriented probe was only slightly contaminated by Fe and Cr. The ratio of the integrated intensities of various peaks with respect to the Mo3d (3d 3/2 and 3d 5/2) peak (after background subtraction) are given in Table I. The ratio of the relative intensities (probe perpendicular / probe parallel) normalized to the respective Mo3d signal are shown in Table II. The Fe and Cr deposited seem to be only partially oxidized as can be seen from Table I and from the peak shapes.

The low impurity concentration on the parallel oriented probe suggests that either there is sputtering on the antenna or more likely there is a low impurity flux in this direction. To determine whether sputtering in this direction is important, further Molybdenum samples, coated with a few Angstroms thick gold layers are presently placed on the bar antenna in TCA.

b) Electrical probe measurements

Figure 3 shows the electron temperature and the ion density profiles during RF heating experiments (P_{RF} = 100 kW) using the stainless steel plate antenna. Compared with the electron temperature during the ohmic heating phase, a temperature increase during the RF is observed. The e-folding length λ_{Te}, before and during the RF pulse, does not significantly change. Similar apparent temperature increases were observed with other RF heating methods such as ICRH /3/. Furthermore, it is noticeable that a strong temperature increase near the limiter radius is observed during the sweep through of the Discrete Alfvén Wave resonance (n,m) = (-2,-1) /6/. There are also indications that during RF the electron temperature increases near to the wall.

Contrary to the scrape-off measurements made during ICRH in TFR, a decrease in ion density is observed. As shown in Fig. 3c, the ion density decreases drastically in the case of the stainless steel antenna. Strong modifications of the density profile within the RF pulse are detected. The e-folding length λ_{ni} increases, and nearly flat density profiles may even be observed.

Edge temperature profile measurements with the TiN-coated bar antenna are presented in Fig. 4. An increase in electron temperature at the same level, as in the case of the stainless steel antenna, is observed and the temperature is roughly comparable with the previous case. However, it seems that in the region of the antenna slightly higher temperatures are encountered. This may be because the plasma becomes non-Maxwellian during the RF phase due to plasma-antenna interactions.

The biggest difference is found in the behaviour of the ion density. Drastic changes, such as strong profile modifications, are not observed. With the bar antennae, the density decrease is still observed, but strongly reduced. Furthermore, a slight density reduction occurs around the antenna radius.

The power dependence of the ion density and electron temperature at different probe positions is shown for the bar antenna in Fig. 5. The electron density at all the probe positions studied decreases roughly linearly with RF power. No such clear cut dependence of the electron temperature has been observed.

The ion temperature at fixed probe positions, measured by means of the Katsumata probe, is shown in Fig. 6. As already seen for the electron temperature, an increase in the ion temperature is observed. The temporal behaviour of the edge ion temperature is very similar to the central ion temperature as measured with the neutral particle analyser.

In the TCA boundary plasma, as in other Tokamak scrape-off layers /12/, large low frequency density fluctuations are observed. The frequency spectrum of these fluctuations, as shown in Fig. 7a, extends up to about 600-700 kHz and the spectral power falls with an approximate power-law dependence $P(f) = f^{-\alpha}$ where α is roughly between 1 and 2 during the RF pulse. Using the spectrum analyser as a narrow band receiver, tuned at 150 kHz, a radial power profile at this particular frequency was established as shown in Fig. 8a. In the ohmic heating phase the low frequency fluctuations at 150 kHz stay at a low level behind the antenna radius but their activity increases as we approach the limiter radius. During the RF heating phase, a peak of low frequency turbulence, which grows in time, is measured in front of the antenna position. Just after the end of the RF pulse, higher fluctuation levels are observed, which expand even into the region between the antenna and the wall. This behaviour of the low frequency turbulence is coupled with profile changes in the scrape-off layer. Figure 8b demonstrates that changes in the gradients of the ion saturation current, which is proportional to the ion density, are related to increasing or peaking fluctuation levels such as shown in Fig. 8a.

High frequency density fluctuations at the driving frequency have also been detected. As well as the fundamental frequency, higher harmonics have been observed (see Fig. 9). Under certain conditions, intermediate frequencies such as $3/2\ \omega$ and $5/2\ \omega$ and higher frequency noise could be measured.

More detailed measurements of density fluctuations at the driving frequency and their harmonics are presently in progress and will be presented later.

The floating potential of a Langmuir probe is very sensitive to fast electron populations. This sensitivity results from the fact that, at the floating potential, the electron current must be balanced by the ion current. Therefore even a small number of fast electrons may drive the floating potential negative. The behaviour of the floating potential in the TCA scrape-off layer is presented in Fig. 8c. During the RF pulse, the floating potential goes negative to about -30V. This fact may indicate the presence of fast electrons during the RF phase. This fast electron population may either be due to heating or to RF-driven electron beams.

A recent study showed that in a large volume, low density plasma during intense RF, hot and cold electron distributions exist /13/. The electron beam, driven by the RF, may in fact lead to an important error in the plasma temperature measurements if it is not recognized and accounted for. A detailed check of the Langmuir characteristics indeed revealed that a hot electron population during RF may exist. Figure 10 shows the measured probe current before and during the RF pulse. These measurements show very different behaviour of the probe current during the ohmic heating phase and the RF phase. In Fig. 11 semi-logarithmic plots of the Langmuir characteristics during RF heating experiments are presented for three different RF powers. During the ohmic heating phase, the straight line indicates that the edge plasma was Maxwellian. In the presence of RF, deviations from the straight line were observed. Under this condition, the edge plasma is non-Maxwellian even at low RF power. There are indications that an electron beam exists under these conditions. The energy of this beam seems to correspond roughly to the observed DC potential change of the antenna. However, large improvements in the time resolution of the probe measurements should be possible in the future, allowing the study of the formation and behaviour of the non-Maxwellian edge plasma during intense RF heating.

The presence of intense electron beams may not only lead to misinterpretation of the probe signals. The electron beam gives rise to an important self-polarisation of the whole antenna structure. Its presence may lead to large sheath potentials, not only of the antenna, but also of the limiters, therefore inducing arcing and sputtering. In particular, ions accelerated through many tens of volts become very efficient at sputtering. Also, direct electron bombardment may contribute to the heavy impurity flux. Furthermore, the electron beam may drive strong plasma instabilities in the scrape-off layer.

The following model is proposed to explain the antenna-plasma interaction. In TCA the antenna system is immersed in the edge plasma and the terminals of each antenna oscillate with an amplitude of about ± 200 V at 2.5 MHz. The antenna, therefore, acts as a large Langmuir probe. When a section of the antenna is biased positively, it draws the electron saturation current. Currents up to about 30 A/cm^2 have been estimated, which represent a considerable power loss. This effect would appear as an additional resistive loading of the antenna and could lead to arcing and melting. When the antenna region is biased negatively the plasma ions are accelerated onto the antenna and sputter very efficiently, leading to a large impurity flux into the plasma. This phenomenon may explain the observed strong plasma-antenna interaction at the antenna edges. Furthermore, this simple model is supported by high frequency measurements of the current flowing into a grounded Langmuir probe. With no plasma there was zero pick-up from the RF antennae. The

RF generator delivers a pure 2.5 MHz sine wave and the measurement is shown in Fig. 12. A superposition of 2.5 MHz and 5 MHz is evident. Current density oscillations of a few A/cm^2 are observed, indicating strong plasma-antenna interaction. The RF currents seem largest near the plasma and show a dip at the antenna radius. Spectral analysis of the probe signals show the presence of several higher harmonics of the driving frequency.

In order to reduce the effects of the edge plasma on the antenna, we are installing lateral TiN-coated screens 5 cm from each side of each antenna group. Their main effect should be to reduce the electron density in the scrape-off layer behind the limiters and so reduce the above effects as much as possible.

3. CONCLUSION

Our results have demonstrated that very detailed measurements are required during intense RF heating experiments.

Our measurements showed that the scrape-off layer reacts sensitively to different antenna designs. Both types of antenna showed an apparent electron and ion temperature increase during the RF phase as also observed in other RF schemes. However, compared with those experiments, we observe a density decrease during the heating phase. The density decrease in the case of the bar antenna scales roughly linearly with applied power. The density profile is most directly affected by the different antenna designs. We propose that the antenna may act as a large Langmuir probe and the resulting intense currents and their associated polarization may lead to impurity fluxes in the plasma. This effect may be reduced by adding side screens.

The interaction of the intense RF field with the edge plasma produces a non-Maxwellian electron distribution. This effect complicates the probe measurements and both careful interpretation and high-frequency electronics are necessary. During the ohmic heating phase and during RF heating, low frequency turbulence exists in the edge plasma. The location of this turbulence correlates with gradients in ion density and electron temperature. High frequency density fluctuations at the driving frequency and their harmonics are also observed.

Acknowledgements

We thank M. Marmillod and the TCA support team for their excellent support and Mr. Ripper for the construction of the probes. Also, the great encouragement from Prof. F. Troyon is highly recognized. The present work was partially supported by the Swiss National Science Foundation.

TABLE I

Line	Sample$_{\perp}$	Sample$_{\parallel}$
Mo3d	1	1
C1s	0,46	0,10
O1s	0,90	0,20
Cr2p	0,36	0,05
Fe2p	3,07	0,25

TABLE II

Line	Sample$_{\perp}$ / Sample$_{\parallel}$
C1s	4,49
O1s	4,53
CR2p	7,79
Fe2p	12,21

Figure Captions

Fig. 1: a) Stainless steel plate antenna group

b) TiN-coated bar antenna

Fig. 2: XPS spectrum of Molybdenum deposition probe fixed on the antenna

a) Sample surface parallel to the plate antenna

b) Sample surface perpendicular to the plate antenna

Fig. 3: Scrape-off parameter profiles for the case of the stainless steel antenna

a) Electron temperature

b) Ion density (before and after RF)

c) Ion density during RF

Fig. 4: Scrape-off parameter profile for the case of the TiN-coated bar antenna

a) Electron temperature

b) Ion density

Fig. 5: Power dependence at 3 different probe positions with bar antenna

a) Ion density

b) Electron temperature

Fig. 6: Edge ion temperature (solid line central ion temperature)

Fig. 7: Low frequency density fluctuations during RF

Figure Captions (cont'd)

Fig. 8: Low frequency fluctuation

a) Density fluctuations at 150 kHz

b) Ion saturation current

c) Floating potential

Fig. 9: High frequency density fluctuations during RF

Fig. 10: Langmuir probe characteristics

Fig. 11: Semi-logarithmic presentation of the Langmuir characteristics for 3 different RF powers

Fig. 12: RF currents on a grounded Langmuir probe

References:

/1/ G.M. McCracken in Course on Diagnostics for Fusion Reactor Conditions Vol. II p. 419, International School of Plasma Physics, Varenna, Commission of the European Communities, Brussels.

/2/ S.J. Zweben and R.J. Taylor, Nucl. Fusion 23, 513 (1983).

/3/ TFR Group, 11th European Conference on Controlled Fusion and Plasma Physics, Aachen, Vol. II, C34, 493 (1983).

/4/ Hofmann et al., accepted for publication in J. Nuclear Materials.

/5/ A.D. Cheetham et al., 11th Symposium on Fusion Technology, Oxford, Vol. 1, 601 (1980).

/6/ R. Behn et al., Plasma Physics 26, 173 (1984).

/7/ De Chambrier et al., Proc. of the 3rd Joint Varenna-Grenoble Int. Symposium, Heating in Toroidal Plasmas, Grenoble, Vol. II, 1117 (1982).

/8/ De Chambrier et al., 4th Int. Symp. on Heating in Toroidal Plasma, Rome (1984).

/9/ K. Odajima et al. Japan J. Appl. Physics, 17, 1281 (1978).

/10/ F.W. Crawford, J. Appl. Phys., 34, 1897 (1963).

/11/ A. Boschi and F. Magistrelli, Il Nouvo Cimento 29, 487 (1963).

/12/ S.J. Zweben and R.W. Gould, Nuclear Fusion 23, 1625 (1983).

/13/ R.W. Schumacher, N. Hershkowith and K.R. McKenzie, J. Appl. Phys. 47, 886 (1976).

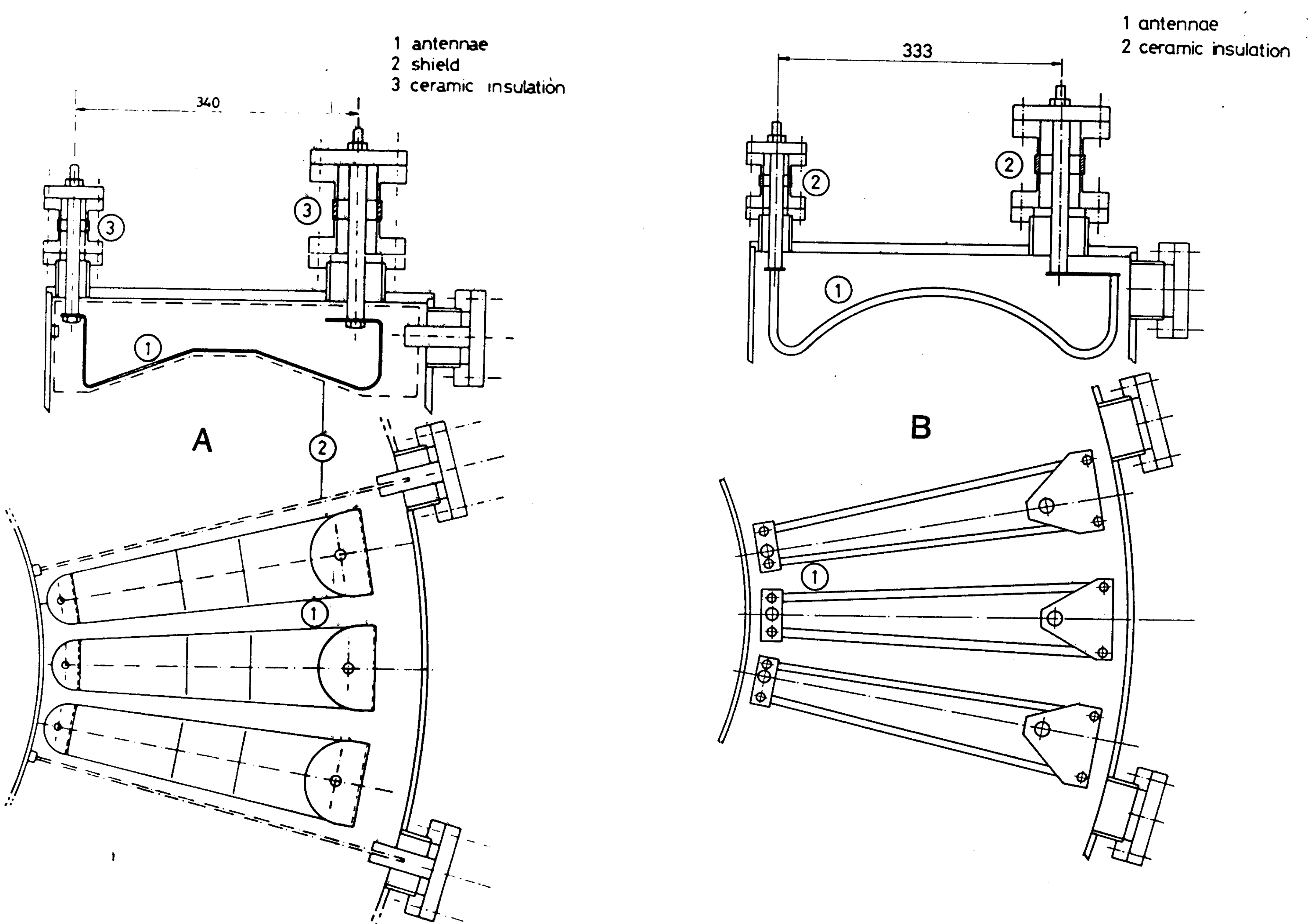

1 antennae
2 shield
3 ceramic insulation
340
A
1 antennae
2 ceramic insulation
333
B

Fig. 1

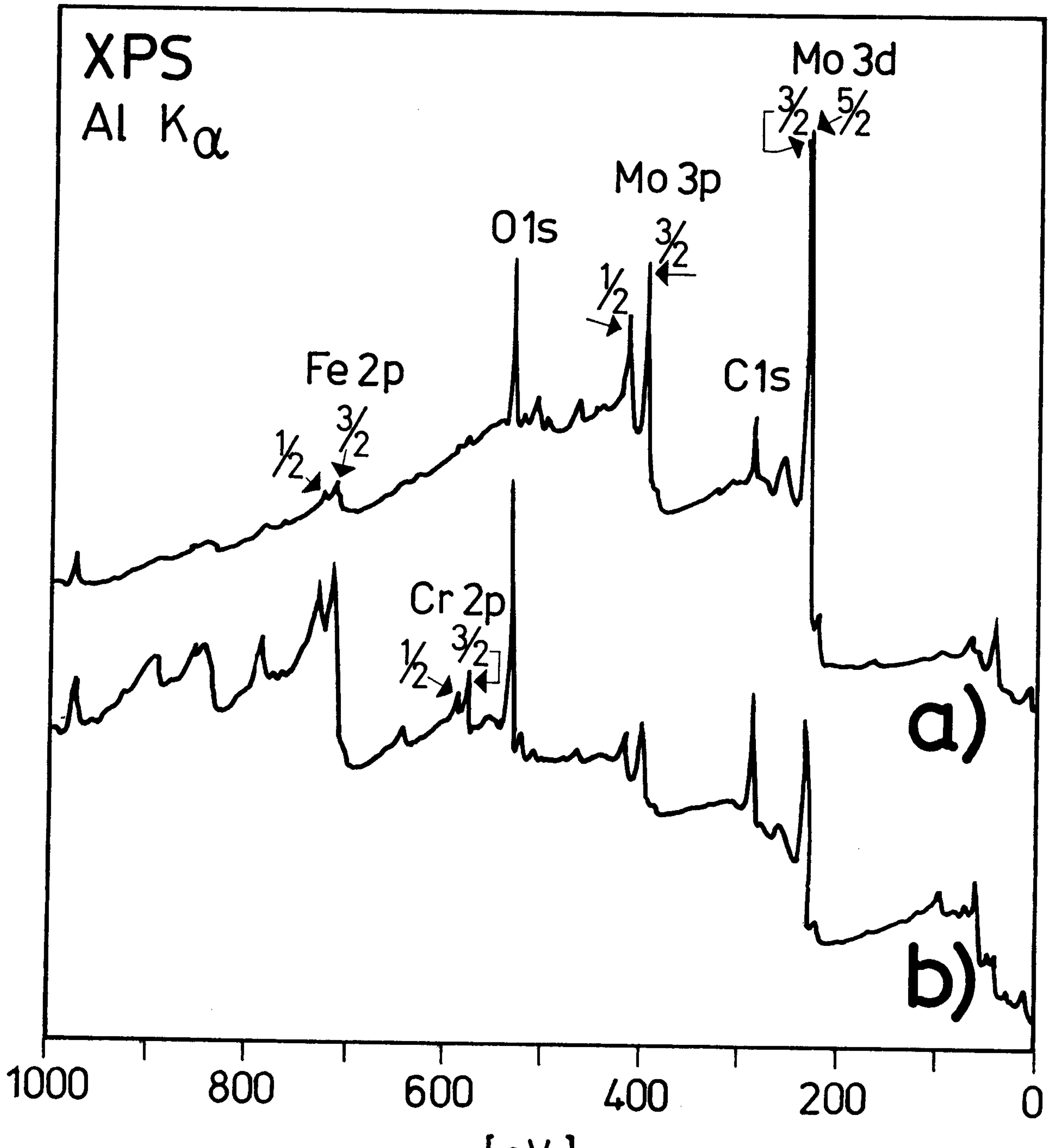
XPS
Al Kα
Mo 3d
3/2
5/2
Mo 3p
3/2
1/2
O 1s
Fe 2p
3/2
1/2
C 1s
Cr 2p
1/2
3/2
a)
b)
1000
800
600
400
200
0
[eV]

Fig. 2

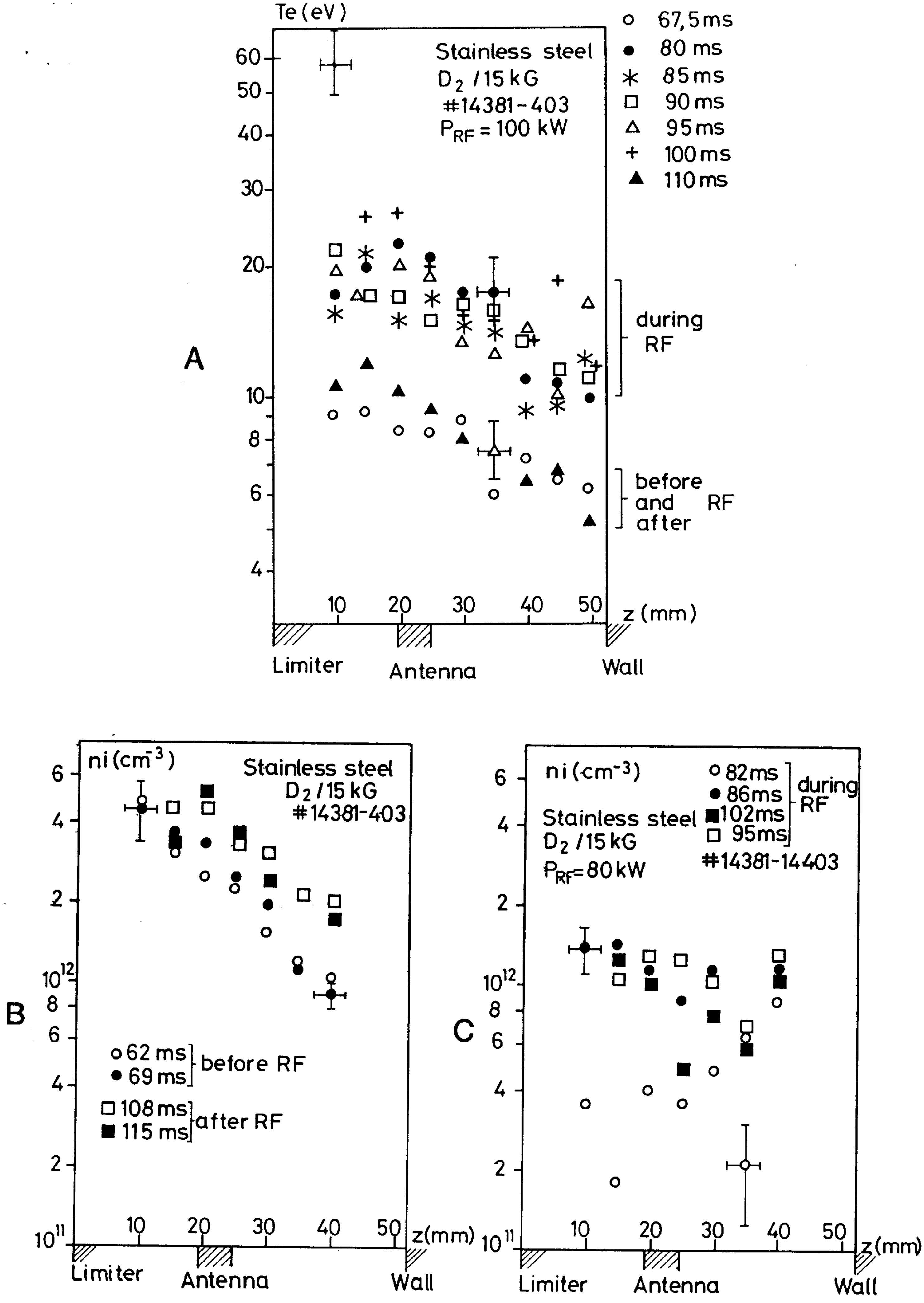
A
Te (eV)
Stainless steel
D_2 /15 kG
#14381-403
P_{RF} = 100 kW
67,5 ms
80 ms
85 ms
90 ms
95 ms
100 ms
110 ms
during RF
before and after RF
z (mm)
Limiter
Antenna
Wall
B
ni (cm^{-3})
Stainless steel
D_2 /15 kG
#14381-403
62 ms
69 ms
before RF
108 ms
115 ms
after RF
z(mm)
Limiter
Antenna
Wall
C
ni (cm^{-3})
82 ms
86 ms
102 ms
95 ms
during RF
Stainless steel
D_2 /15 kG
P_{RF}= 80 kW
#14381-14403
z(mm)
Limiter
Antenna
Wall

Fig. 3

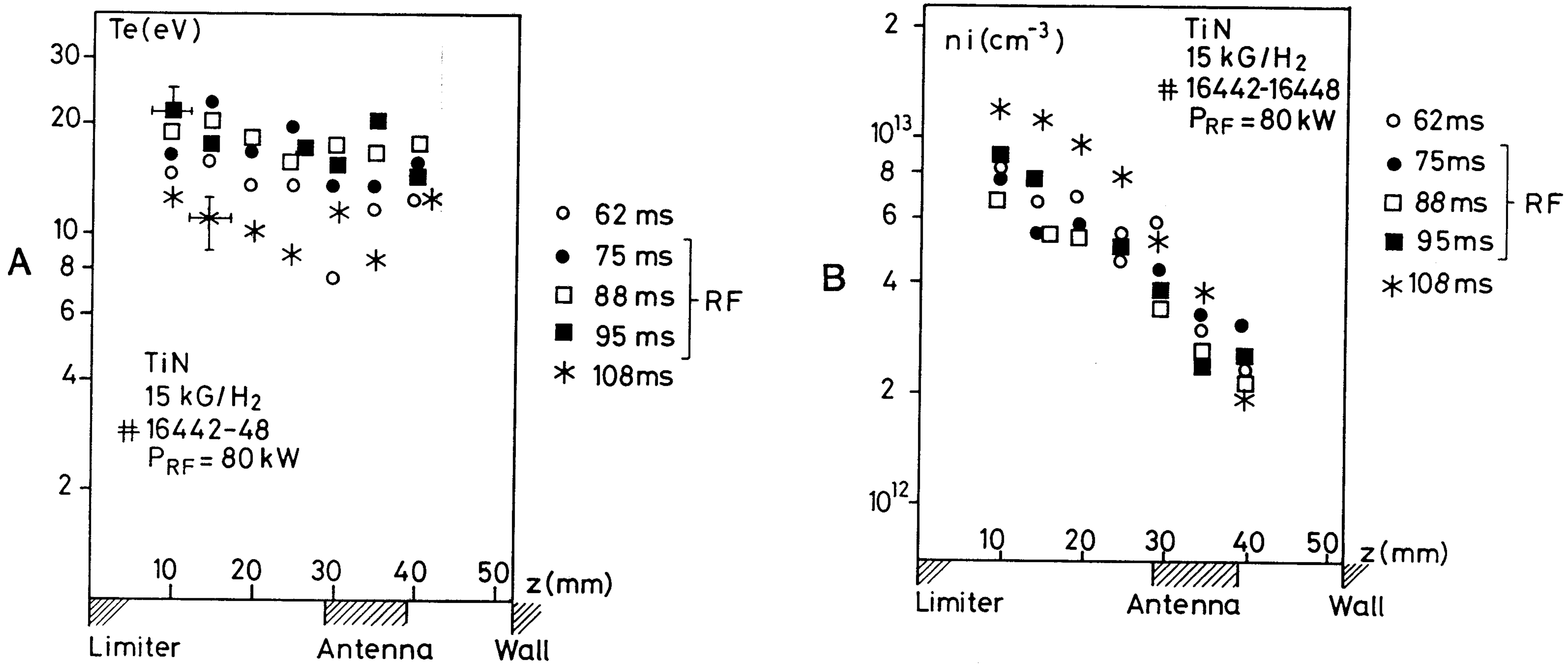
A
Te(eV)
30
20
10
8
6
4
2
TiN
15 kG/H_2
16442-48
P_{RF} = 80 kW
10
20
30
40
50
z(mm)
Limiter
Antenna
Wall
62 ms
75 ms
88 ms
95 ms
108ms
RF
B
ni(cm^{-3})
2
10^{13}
8
6
4
2
10^{12}
TiN
15 kG/H_2
16442-16448
P_{RF} = 80 kW
10
20
30
40
50
z(mm)
Limiter
Antenna
Wall
62ms
75ms
88ms
95ms
108ms
RF

Fig. 4

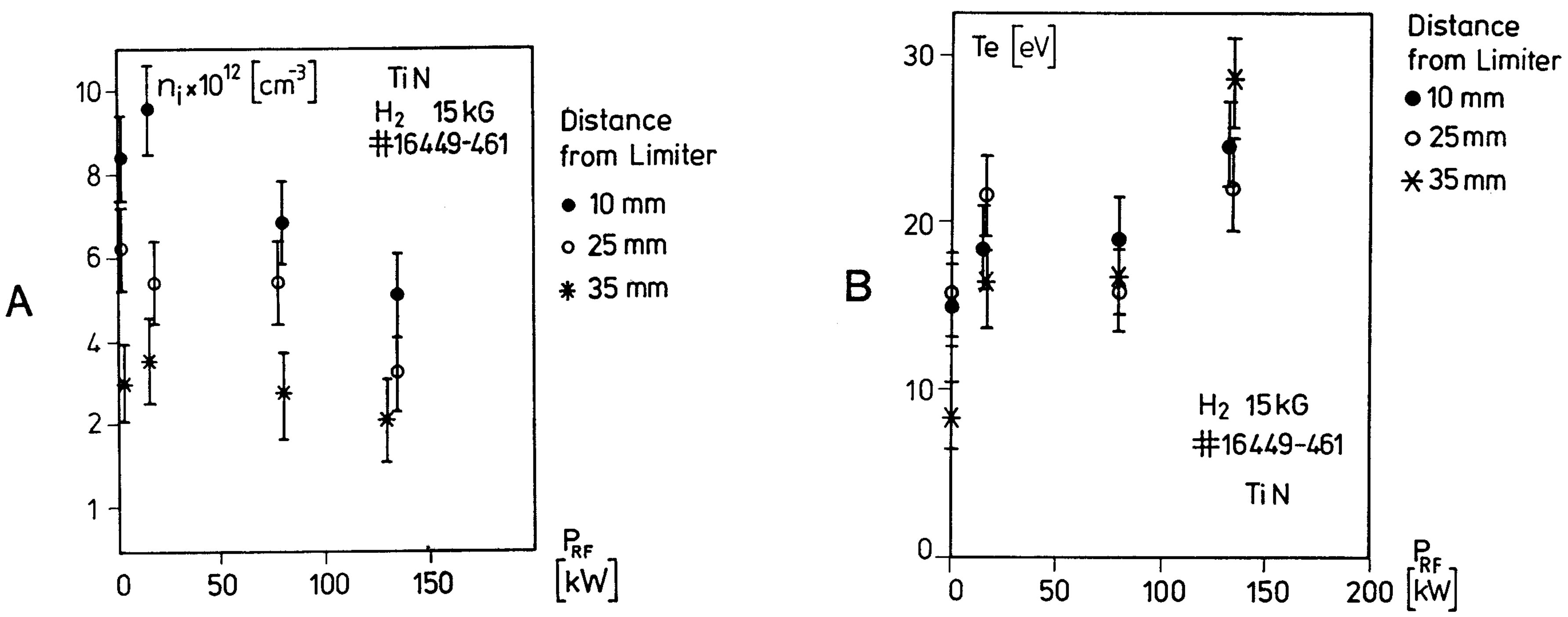
A
n_i x 10^12 [cm^-3]
TiN
H2 15 kG
#16449-461
Distance
from Limiter
10 mm
25 mm
35 mm
P_RF [kW]
B
Te [eV]
H2 15 kG
#16449-461
TiN
Distance
from Limiter
10 mm
25 mm
35 mm
P_RF [kW]

Fig. 5

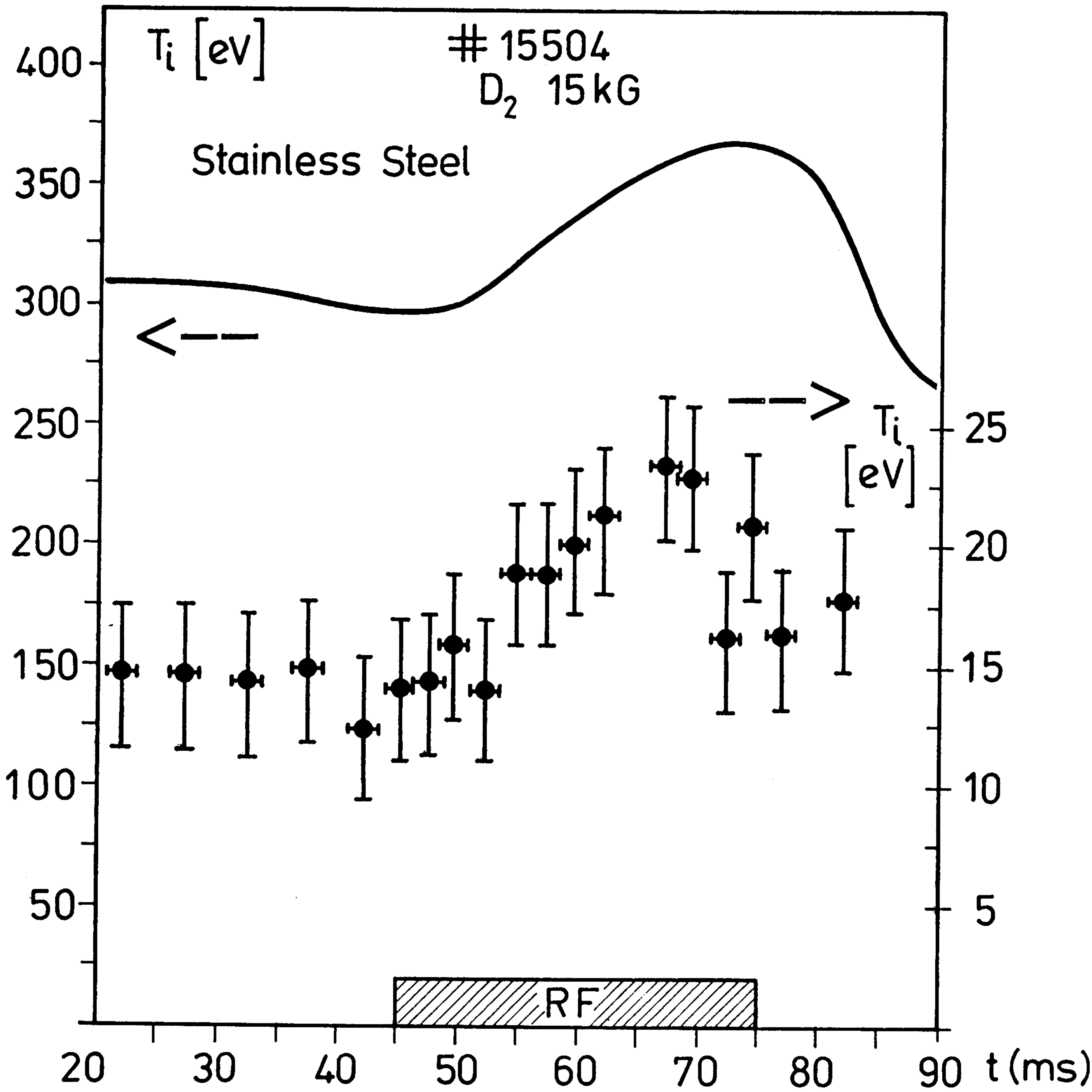

Ti [eV]
15504
D2 15kG
Stainless Steel
Ti [eV]
RF
t (ms)
400
350
300
250
200
150
100
50
25
20
15
10
5
20
30
40
50
60
70
80
90

Fig. 6

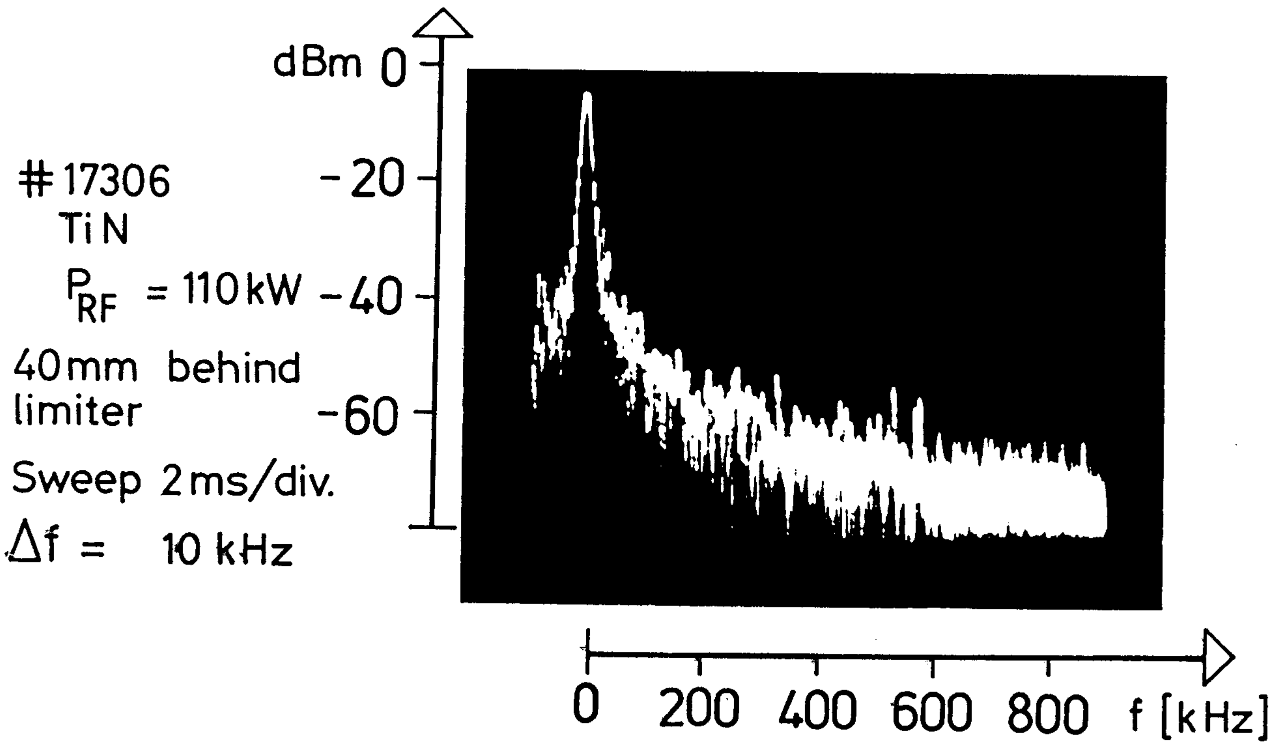

dBm 0
-20
-40
-60
17306
Ti N
P_{RF} = 110 kW
40 mm behind
limiter
Sweep 2 ms/div.
Δf = 10 kHz
0
200
400
600
800
f [kHz]

Fig. 7

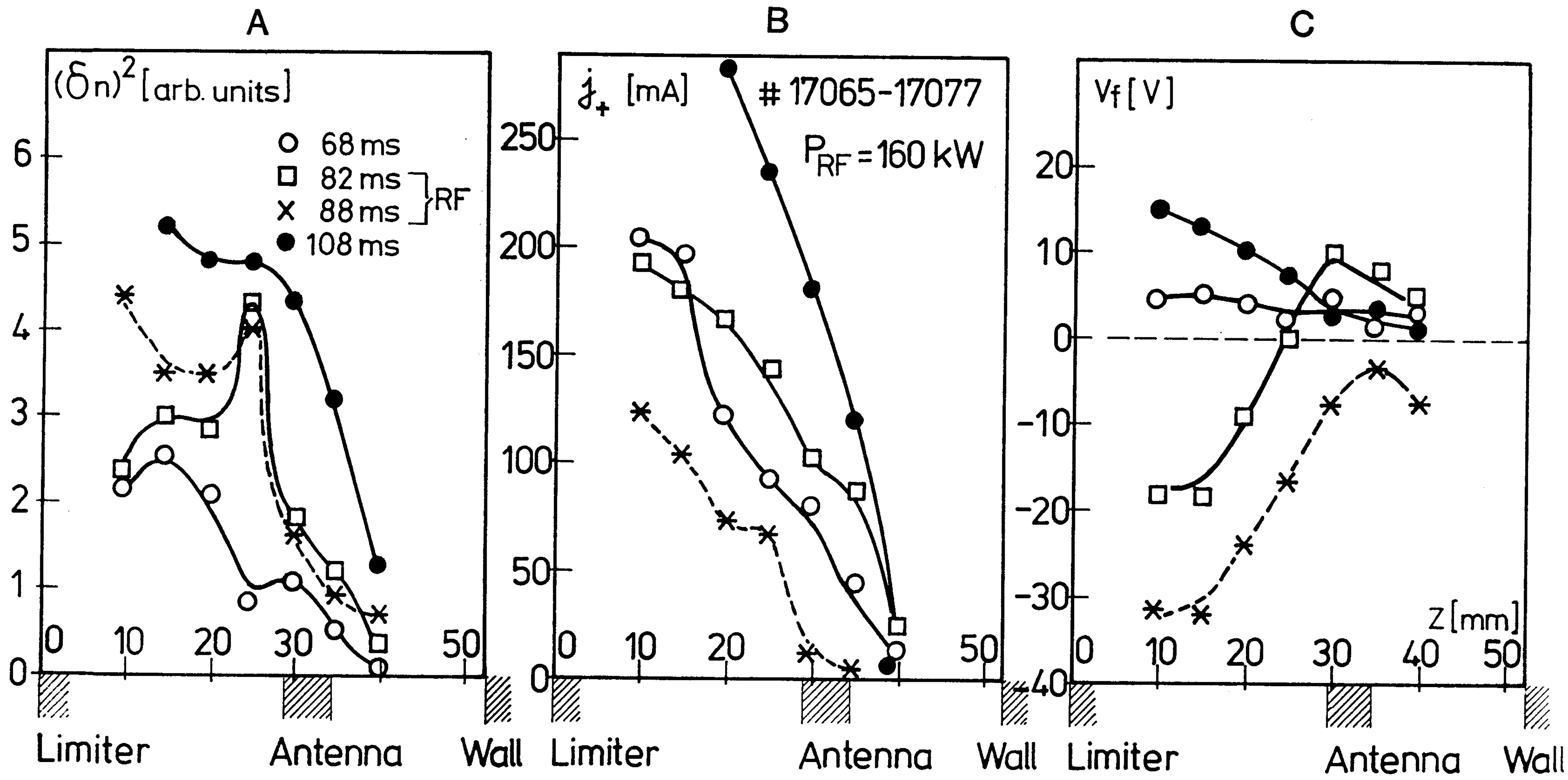
A
B
C
$(\delta n)^2$ [arb. units]
68 ms
82 ms
88 ms
108 ms
RF
j_+ [mA]
17065-17077
P_{RF} = 160 kW
V_f [V]
z [mm]
Limiter
Antenna
Wall

Fig. 8

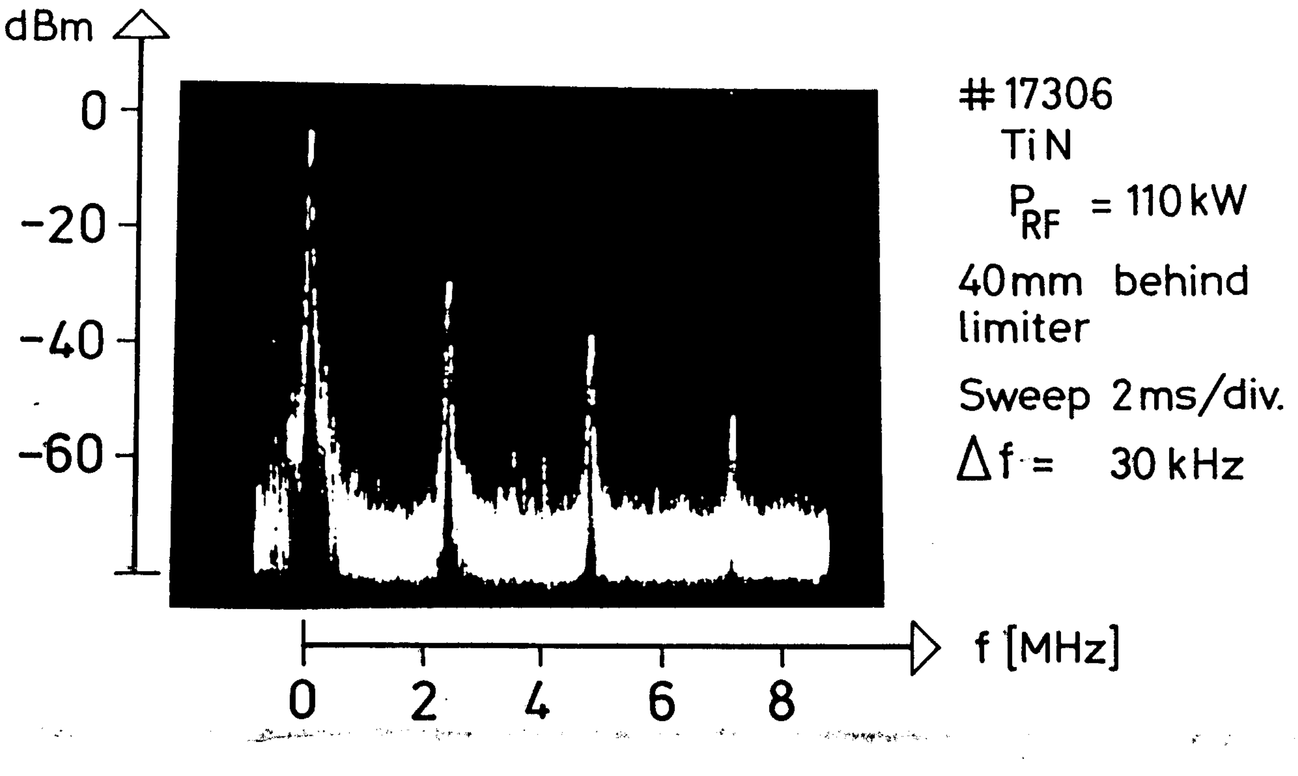
dBm
0
-20
-40
-60
17306
TiN
P_{RF} = 110 kW
40mm behind limiter
Sweep 2ms/div.
Δf = 30 kHz
f [MHz]
0
2
4
6
8

Fig. 9

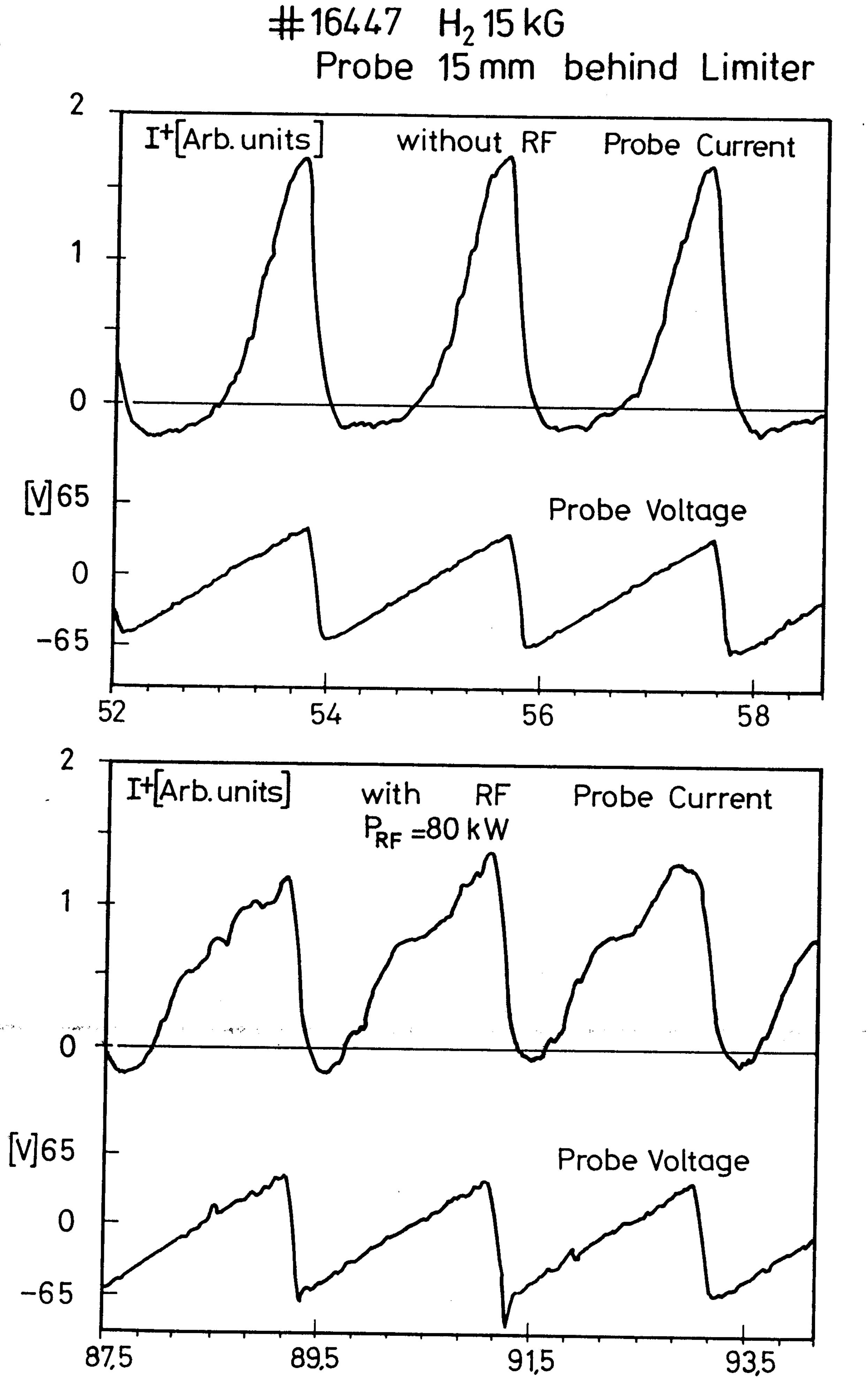
#16447 H_2 15 kG
Probe 15 mm behind Limiter
I+[Arb. units]
without RF
Probe Current
Probe Voltage
[V] 65
0
-65
2
1
0
52
54
56
58
I+[Arb. units]
with RF
P_{RF} =80 kW
Probe Current
Probe Voltage
87,5
89,5
91,5
93,5

Fig. 10

Fig. 11

H_2 15 kG - Probe position 22 mm behind Limiter

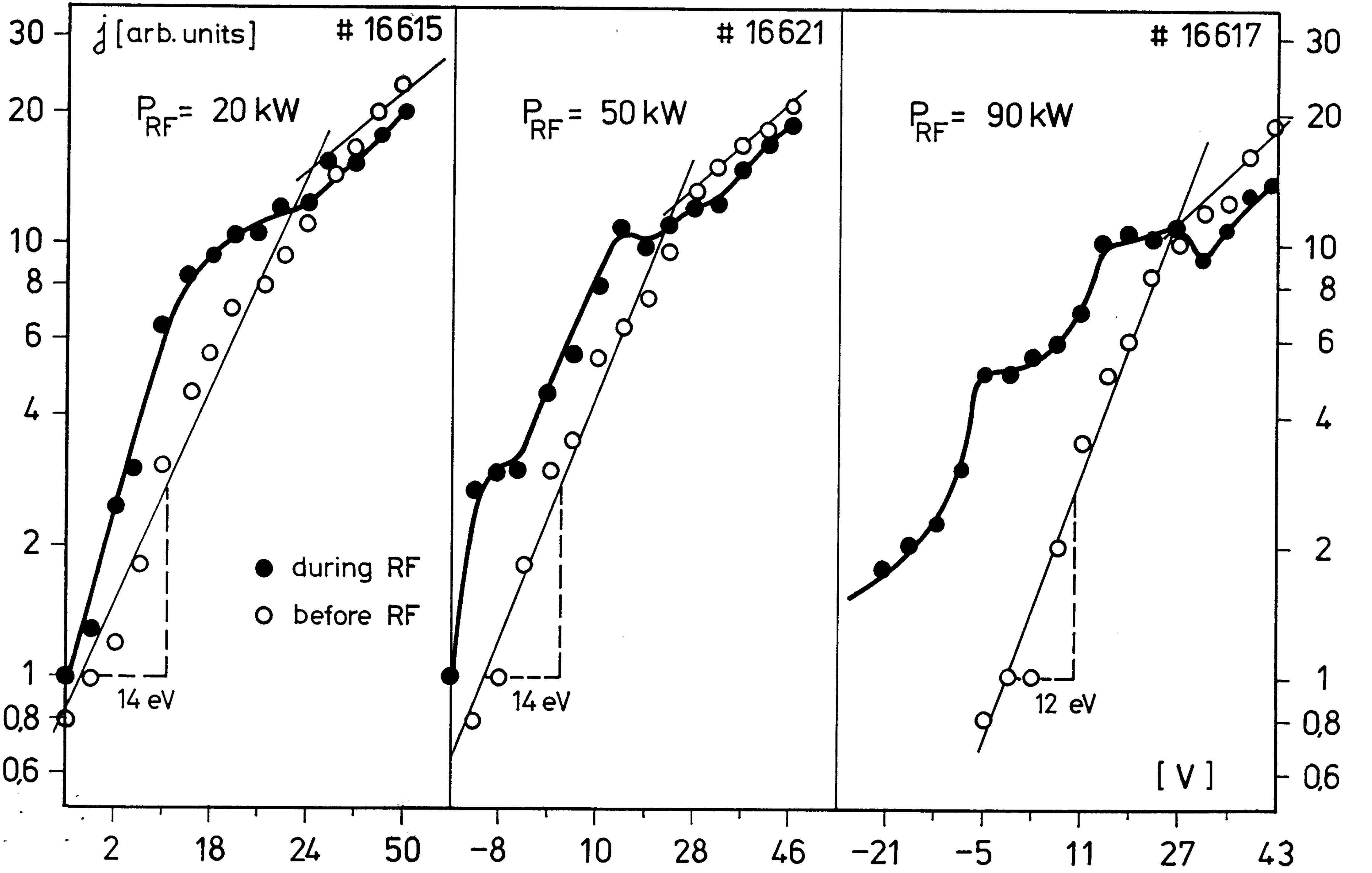

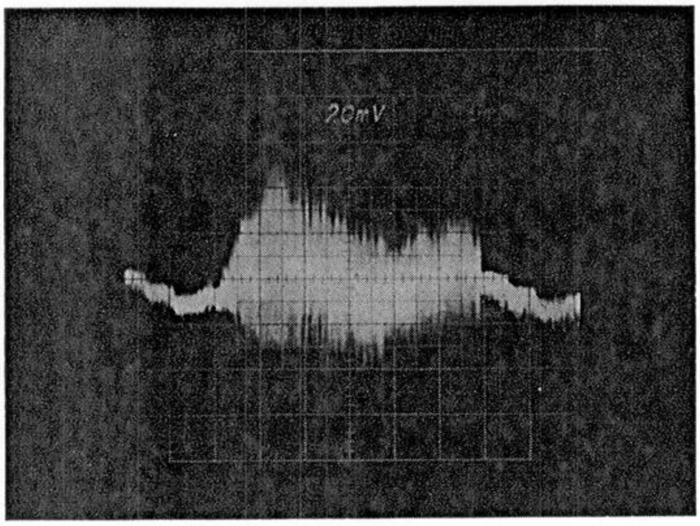

Shot 15912

(stainless steel)

Plasma side of antenna

x= 5 ms/div

y= 2A cm^{-2}/div

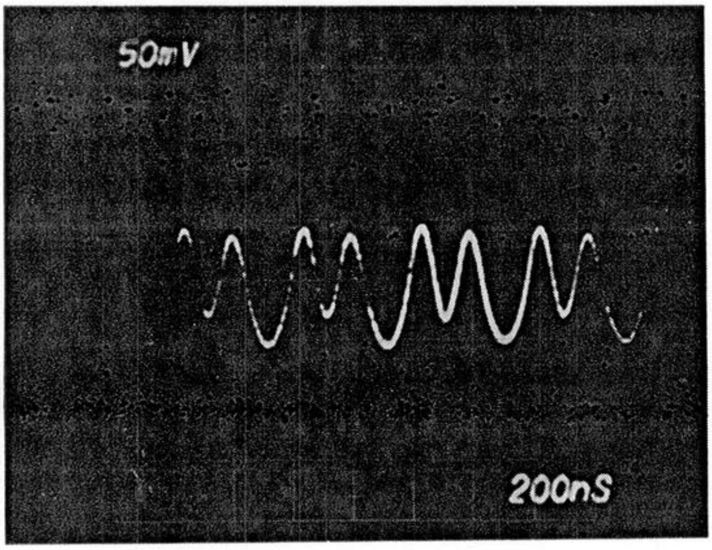

Shot 16402

(TiN)

at antenna position

x= 200 ns/div

y= 5A cm^{-2}/div

Fig. 12